arXiv:hep-ex/9908023v1 8 Aug 1999

BONN-HE-99-04
August 1999

Results on Diffractive Processes from the HERA Collider Experiments[a]

James A. Crittenden
Physikalisches Institut, University of Bonn, Nußallee 12, 53115 Bonn, Germany

We review topical results on diffractive processes from the experiments H1 and ZEUS at the HERA electron-proton collider. Emphasis is placed on the phenomenological and experimental consequences of the discoveries at HERA for the proposed electron/polarized-ion collider EPIC.

1 Introduction

The technical feasibility and experimental program of an electron/polarized-ion collider such as the proposed EPIC collider were studied in detail during the years 1995-1997.[1] During these very years, discoveries at the first electron-proton collider facility ever built, the HERA accelerator complex at the DESY laboratory in Hamburg, Germany, were establishing a new field of study in strong-interaction physics: that of hard diffractive processes.[2] Thus, these initial considerations of the physics motivation for a collider such as EPIC could not fully benefit from the information provided by measurements at HERA now available, just as was the case for the proposed experimental program at the HERA collider itself prior to its operation.[3] It is the purpose of this report to summarize these results from the HERA collider experiments H1 and ZEUS, placing particular emphasis on lessons learned about the physics impact of the results, which we now know to provide valuable insight into the dynamics of the strong interaction, and concerning the experimental requirements for such measurements. We will see that experiments at the proposed EPIC collider would provide essential information complementary to that obtained from investigations at HERA, profiting from the experience at this first electron-proton collider such as to greatly extend the sensitivity to a wide variety of aspects of strong-interaction dynamics inaccessible by other means.

For the purposes of our discussion, we assume the EPIC machine to collide 4 GeV electrons with 40 GeV protons, achieving instantaneous luminosities of at least 10^{33} cm^{-2} s^{-1} which is approximately two orders of magnitude greater than that presently reached at HERA. The electron-proton center-of-mass energy, $\sqrt{s}$, will be therefore 25 GeV, which is also the kinematic limit of the virtual-photon/proton center-of-mass energy, W. Such high luminosity will

[a] Talk presented at the EPIC'99 Workshop on Physics with an Electron/Polarized-Ion Collider, Indiana University Cyclotron Facility, 8-11 April 1999, Bloomington, Indiana, USA

permit investigation of a range in photon virtuality, Q^2, extending well into the perturbative regime. Of particular interest is the recently identified transition region $0.1 \lesssim Q^2 \lesssim 1$ GeV.[2] Assuming a central detector geometry with a beam aperture of a few centimeters, located approximately 1 m from the interaction point in the rear direction (the electron flight direction), the scattered electron will be detected in to the central detector for this range in photon virtuality, obviating the need for special-purpose electron detectors. The Lorentz factor of the center-of-mass system in the laboratory frame at EPIC will be 1.6, less severe than the factor 2.7 at HERA. This will ease the constraints on the very forward detectors employed to distinguish exclusive from proton-dissociative diffractive processes, but will require excellent tracking and calorimetry in the rear direction in order to cover the photon fragmentation region with good resolution. The rapidity range covered at EPIC will be approximately 3 units less than the 9 units available at HERA, with negative consequences for inclusive studies dependent upon rapidity gap requirements, especially studies of jet production. On the other hand, the EPIC kinematics are ideal for investigations in the rapidly-growing field of exclusive and semi-exclusive processes, such as vector-meson photo- and electroproduction.[4] Of particular interest are measurements of the helicity structure of these diffractive processes, and the ability to polarize the electron and proton beams allow EPIC to play a unique rôle in its elucidation. Thus, the center-of-mass energy sufficient to reach the diffractive regime, and to produce all of the vector mesons, along with the high luminosity and the ability to survey the transition region in photon virtuality ensure a rich physics program for EPIC. We omit discussion of the additional investigations of QCD effects made possible by the acceleration of ion beams, since they have not yet been addressed by measurements at HERA.[5,6,7]

2 Phenomenological Issues

The phenomenological success of Regge theory in describing diffractive interactions is well established.[8] However, the past 25 years have produced persuasive experimental evidence that the fundamental structure of the strong interaction is described by the quantum field theoretical treatment implemented in Quantum Chromodynamics (QCD). A thorough understanding of the relationship between these two approaches remains elusive and its attainment is viewed as one of the primary goals of contemporary particle-physics research. The H1 and ZEUS collaborations have invested major efforts in characterizing the kinematic regions of validity of these two highly disparate views of the strong interaction, and in measuring the transition between the two regimes.[9]

Regge theory leads to various scaling laws which sharply distinguish it from the quantum chromodynamical description. The energy dependence of forward

scattering cross sections is characteristically weak, scaling as a power law with a power of 0.32, which corresponds to the intercept of the Pomeron trajectory determined in hadronic interactions [10]: $\alpha(t) = 1.08 + 0.25\ t$. Gribov [11] showed that the observed steeply forward peaking of the differential cross section $\frac{\mathrm{d}\sigma}{\mathrm{d}t}$ may be expected to increase logarithmically with energy as a consequence of unitarity and the analyticity of the scattering amplitudes. This latter phenomenon is often referred to as "shrinkage", and has been verified experimentally for a wide variety of diffractive interactions, including the soft diffractive photoproduction of vector mesons.

The past few years have seen rapid progress in the theoretical understanding of diffractive processes in the framework of QCD, including a number of impressive phenomenological successes. Diffractive processes are modeled as proceeding via the exchange of a coherent pair of gluons in a color-singlet state, as proposed early in the development of QCD.[12] Figure 1 shows a diagram for exclusive vector-meson electroproduction which exemplifies such models.

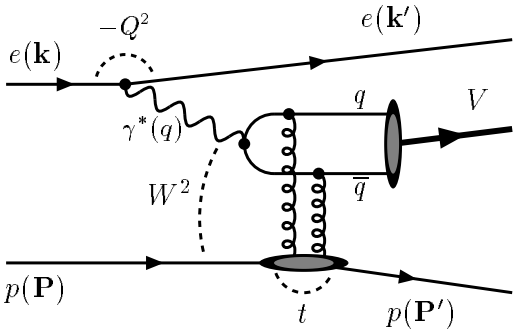

Figure 1: Schematic diagram illustrating exclusive vector-meson electroproduction as mediated by the exchange of a gluon pair in a color-singlet state

Among the many consequences of such a model are the steepening of the energy dependence of the forward cross section with increasing photon virtuality due to the gluon density in the target, and the energy independence of the forward peaking.[13] Of particular interest for the study of exclusive and semi-exclusive meson production are the specific predictions that the final-state meson be longitudinally polarized,[14,15,16,5,17] and that small helicity-violating effects are to be expected.[18,19]

Of essential import for these calculations is the identification of the scale associated with each type of interaction. The rôle of various kinematic quantities in reaching the asymptotically free regime characteristic to QCD is under active

investigation at HERA. The photon virtuality,[20,21] the vector-meson mass in exclusive photo- and electroproduction of vector mesons [22,23] and the momentum transferred to the target in exclusive and semi-exclusive processes [24,15,16] have each been proposed as scale variables The collider experiments at HERA are sensitive to the transition region in each of these variables, as will be the experiments at the EPIC collider.

3 Total γ^*p cross section

In order to study the transition from the soft to the hard regime of photon virtualities in the inclusive deep-inelastic electron-proton scattering process, a definition for the total cross section for virtual-photon/proton interactions is required. It is obtained by adopting a convention for the virtual-photon flux from the electron beam [25] in order to relate the $\gamma^* p$ cross section to the ep cross section. Such a definition makes physical sense if the lifetime of the virtual photon is sufficiently long that the photon traverses two proton radii. One can show that this condition corresponds to values for the Bjorken scaling variable x less than 0.06.[26,23,4] In this low-x region, x may be approximated by $x \simeq Q^2/W^2$, and the total cross section is related to the proton structure function $F_2(x, Q^2)$ via

$$\sigma^T_{\gamma^* p} + \sigma^L_{\gamma^* p} \approx \frac{4\pi^2\alpha}{Q^2(1-x)} F_2(x, Q^2), \tag{1}$$

where the photon-proton cross section has been expressed as the sum of its contributions from longitudinal and transverse photons, and α is the fine structure constant. Figure 2 compares the photon-proton total cross sections for real and virtual photons over the entire region covered by fixed-target experiments and by the collider experiments at HERA, along with a dashed line representing the condition $x = 0.06$. At high photon virtuality, the HERA results extend from the region where this condition no longer holds, and the cross section falls rapidly with increasing x, to the region where the cross section is steeply rising with energy, driven by the gluon density in the proton. The total cross section for real photons at high energy exhibits the weak energy dependence characteristic of models based on Regge theory. The dearth of measurements in the kinematic region to be covered by the EPIC collider clearly shows the need for further measurements in this region of transition between nonperturbative and perturbative behavior.

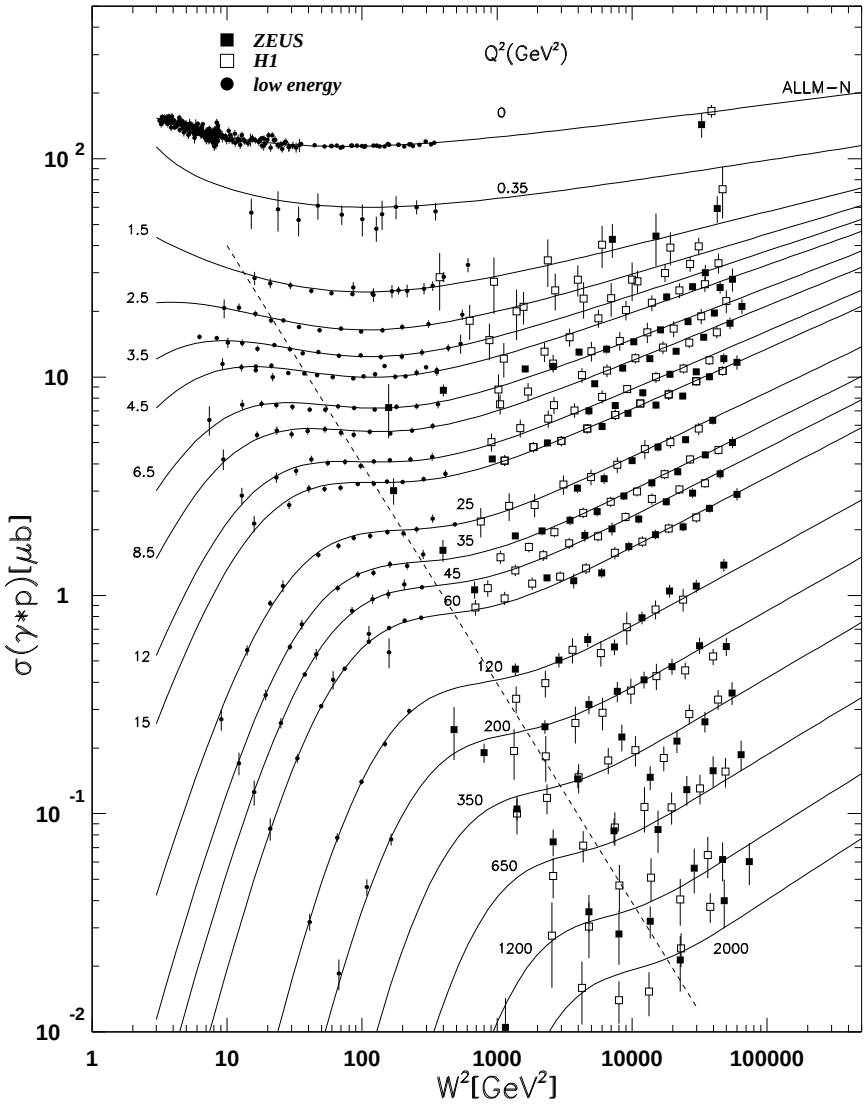

Figure 2: Total photon–proton cross section, $\sigma(\gamma^* \mathrm{p})$, as a function of the squared center-of-mass energy for various values of Q^2 as measured by the ZEUS [27] and H1 [28] collaborations and by the NMC collaboration [29] at CERN. The curves represent calculations using the ALLM proton structure function parametrizations.[30] The dashed line connects points where x=0.06

4 Diffractive contribution to the total γ^*p cross section

The initial observation of a hard diffractive process at HERA was made during the early analyses of the proton structure function F_2. Data selection criteria related to the forward direction were found to reject a category of events which were not present in the available simulations. An event candidate exemplifying this subcategory of the total photon-proton cross section is shown in Fig. 3.

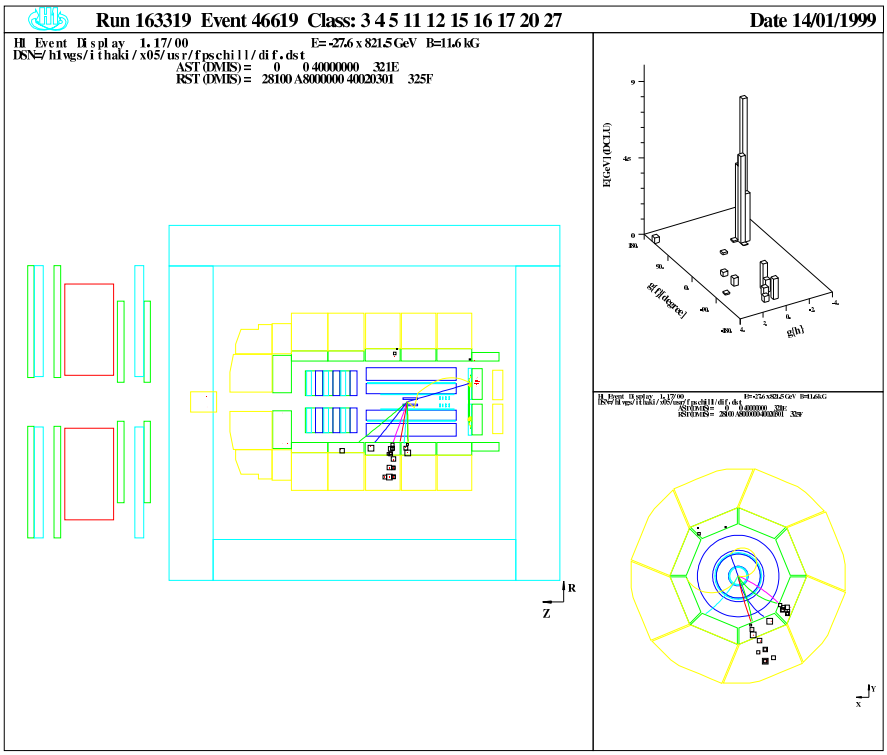

Figure 3: Event recorded by the H1 detector exhibiting a diffractive topology with a rapidity gap between the photon fragmentation region and the forward direction

These events exhibit a rapidity gap between the most forward energy deposit in the central detector and the proton flight direction. A distribution in this event variable, dubbed $\eta_{\max}$, is shown in Fig. 4, together with the results of simulations of the diffractive (POMPYT) and nondiffractive (ARIADNE) components. The absence of event activity between the target and photon

fragmentation regions is used to characterize event topologies arising from this inclusive diffractive process, since it indicates the absence of color flow and hence the exchange of a colorless object as the underlying production mechanism.

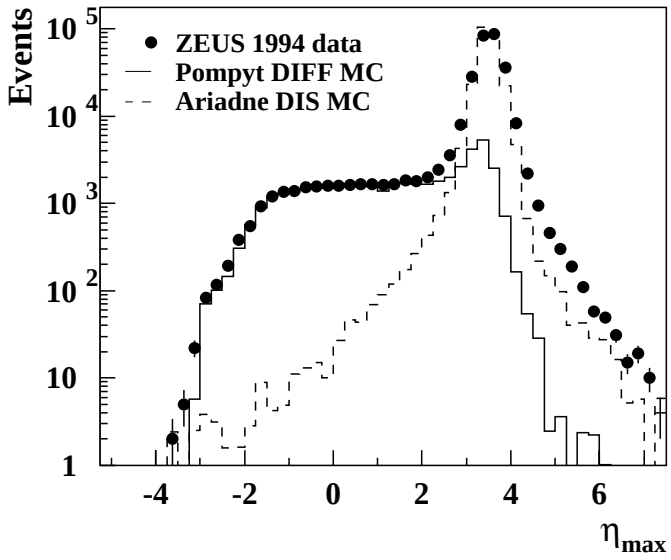

Figure 4: Sample distribution in $\eta_{\max}$, the rapidity of the most forward energy deposit, compared to simulations distinguishing the diffractive component in the inclusive electroproduction process

This means of isolating a clean sample of diffractive events is supplemented in the ZEUS [31] and H1 [32] experiments by trigger selection criteria based on forward baryon detectors. The identification of a forward proton or neutron provides a very clean technique for isolating the diffractive component. Measurement of the baryon momentum provides further information on the dissociation of the initial-state proton. Each of the experiments operates both a forward proton spectrometer and a forward neutron calorimeter. Such detector components will be essential for the study of diffractive physics at the EPIC collider, since the rapidity-gap selection technique will suffer from the limited rapidity range at the lower energy. The strict requirements on such detectors, which include extreme radiation conditions, very accurate momentum measurement, and excellent angular resolution at very small production angles impose the necessity of close interaction with the accelerator physicists

during both the design and operation phases. For example, the calibration of the ZEUS leading-proton spectrometer, which consists of silicon-strip detectors in Roman pots, depends crucially on accurate knowledge of the geometry of beam-line components and their magnetic fields, and its operation is possible only under clean background conditions which are very sensitive to the proton-beam injection procedure. The design of experiments for diffractive physics at the EPIC collider will thus profit greatly from the experience gained at HERA.

5 Exclusive processes

The data obtained by the HERA collider experiments during their first six years of operation have proven them to be excellent sources of information on exclusive strong processes. Such investigations cannot be performed at pp or $p\overline{p}$ colliders, where the acceptance of the central detector components is limited to interactions producing high transverse energy in the final state, or at e^+e^- colliders, where the primary interaction is electroweak. The electron-proton collider geometry has thus been shown to result in sensitivity to a rich variety of strong-interaction phenomena inaccessible by other means. The excellent solid-angle coverage of the H1 and ZEUS central detectors, along with simple special-purpose scintillation counters in the forward region, permits selection of the exclusive reaction $ep \to epV$, where V is a vector meson (ρ^0, ω, ϕ, J/ψ, Υ), with the background from proton-dissociative processes limited to less than 20%.[4] (The latter semi-exclusive process has sparked much theoretical interest recently and will be discussed in Sect. 6.) Of particular interest to instrumentation experts is the necessity of a low-noise nearly-hermetic central calorimeter to provide high-resolution event criteria for exclusivity in such studies. These diffractive processes offer three variables as tunable gauges for the scale of the interaction: Q^2, M_V and t, and thus hold great promise for tests of QCD models of diffraction. The kinematically required minimum transverse kick means that the parton density functions are necessarily skewed, with the skewedness parameter, $\delta \equiv (x_1 - x_2)$, given by

$$|t|_{\rm min} = m_{\rm p}^2 \, \frac{(M_V^2 + Q^2)^2}{W^4} \;=\; m_{\rm p}^2 \, \delta^2. \tag{2}$$

It has been shown recently that the comparison of exclusive J/ψ and Υ photoproduction cross sections yields information on the evolution of the skewed gluon density in the proton.[33,34] In the following, we give examples of HERA measurements which demonstrate the choice of scale parameter by distinguishing data samples of low and high photon virtuality.

5.1 *Exclusive photoproduction of vector mesons*

The central detectors of the H1 and ZEUS experiments are efficient for the detection of the scattered electron for photon virtualities exceeding about 4 GeV^2. A simple signature for the exclusive photoproduction of vector mesons is thus the reconstruction of the decay products in the central detector in the absence of any other energy deposits. Indeed, the first exclusive reaction cross section measured at HERA was that for the photoproduction of ρ^0 mesons,[35] owing to its large cross section (10 μb, about 7% of the total photon-proton cross section) and simple event topology. These measurements, as well as those that followed for the ϕ and ω mesons, exhibited the weak energy dependence and steeply forward peaking characteristic to soft diffractive processes. Figure 5 shows the energy dependence of the exclusive photoproduction cross sections for the light vector mesons, comparing it to that of the total photon-proton cross section and to that observed in exclusive J/ψ photoproduction.[36] The

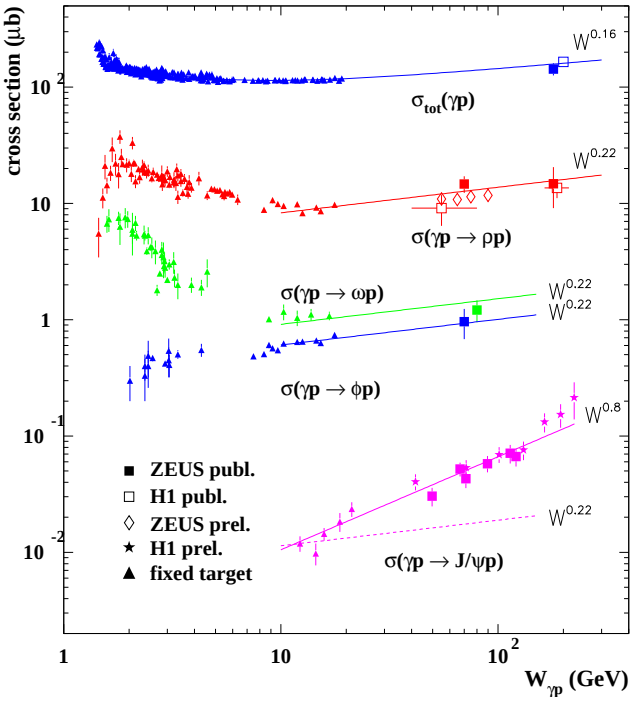

Figure 5: Measurements of the exclusive photoproduction cross sections for ρ^0, ω, ϕ and J/ψ mesons versus energy, compared to the total γp cross section. The lines indicate the slopes of three types of power-law dependence

power of 0.32 (see Sect. 2), expected for the forward cross sections according to Regge phenomenology, is reduced to 0.22 by the integration over t and the energy dependence in the Pomeron trajectory. The much steeper energy dependence observed in J/ψ photoproduction is consistent with the prediction of Ryskin[22] and has inspired efforts to extract the gluon density in the proton from these measurements.[37] The measurements from fixed-target experiments at $W \simeq 10$ GeV indeed served as the initial indication that the energy dependence was strong but the kinematics and statistics of those measurements precluded a variety of further studies (t dependence, decay-angle analyses) which will be made possible by the EPIC collider.

As mentioned in Sect. 2, one means of characterizing the underlying production process in the exclusive photoproduction of vector mesons is given by studying the energy dependence of the forward peaking. In the framework of Regge phenomenology, such a dependence arises from the t dependence of the Pomeron trajectory: $\alpha(t) = 1.08 + 0.25\ t$. Such a dependence is not expected in models which assume the exchange of a pair of gluons in a color-singlet state.[13] Its study requires high experimental sensitivity, since the dependence on energy is logarithmic. At present, the range of energy available to the H1 and ZEUS experiments has not sufficed to accurately measure such shrinkage effects, motivating attempts to include low-energy data in the analysis.[38,39] Figure 6 shows the result of such an investigation by the ZEUS collaboration[39] for exclusive photoproduction of ρ^0 mesons. By restricting the low-energy data to that of the OMEGA experiment[43] in order to exclude data at $W < 8$ GeV, which suffer from contamination of the Pomeron exchange mechanism by other exchange mechanisms,[44] this analysis achieves a clear measurement of the t dependence, covering a t range in which the energy dependence evolves from rising to falling. The Pomeron trajectories determined for the ρ^0 and ϕ via this method are shown in Fig. 7, along with the results of fits illustrating the type of t dependence observed. The observed t dependence is weaker than that extracted from the Donnachie-Landshoff parametrization of hadronic cross sections.[10,45] Of particular interest will be the extension of these investigations to higher momentum transfer, in order to identify a transition to a regime where perturbative exchange mechanisms apply. For such studies, further measurements at $W \gtrsim 10$ GeV are necessary. Furthermore, an initial analysis of this effect in J/ψ photoproduction has yielded the conclusion that such a t dependence is absent and thus that the underlying exchange mechanism is consistent with the perturbative expectation and inconsistent with Regge phenomenology.[38] Unfortunately, the lack of low-energy data required the use of measurements performed using a muon beam on an iron target,[46] rendering the result controversial, owing to uncertainties associated

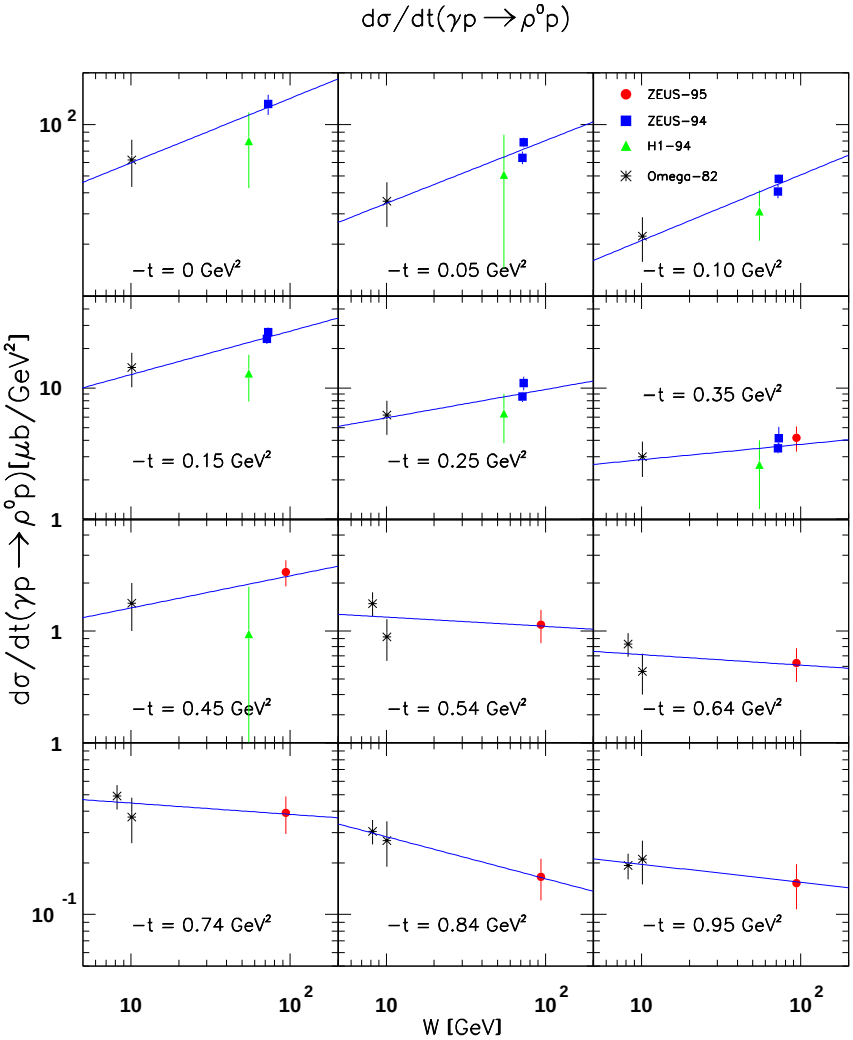

Figure 6: Exclusive ρ^0 photoproduction cross sections as a function of the photon-proton center-of-mass energy, W, for various values of t. The analysis compares the measurements by the H1 [40] and ZEUS [39,41,42] collaborations at high energy to those performed at low energy by the OMEGA experiment.[43] The error bars show the quadratic sum of statistical and systematic uncertainties. The lines indicate the results of fits to the form $\frac{\mathrm{d}\sigma}{\mathrm{d}t} \propto (W^2)^{2\alpha(t)-2}$ performed in order to determine the parameters of the Pomeron trajectory

with nuclear effects.[47] Investigations restricted to the HERA energy regime alone lack the sensitivity to rule out the shrinkage effect at the level observed for the light vector mesons.[36] Here again, a clear understanding of this issue, and the associated measurement program to further investigate the dynamics of the production process require measurements in the EPIC energy range.

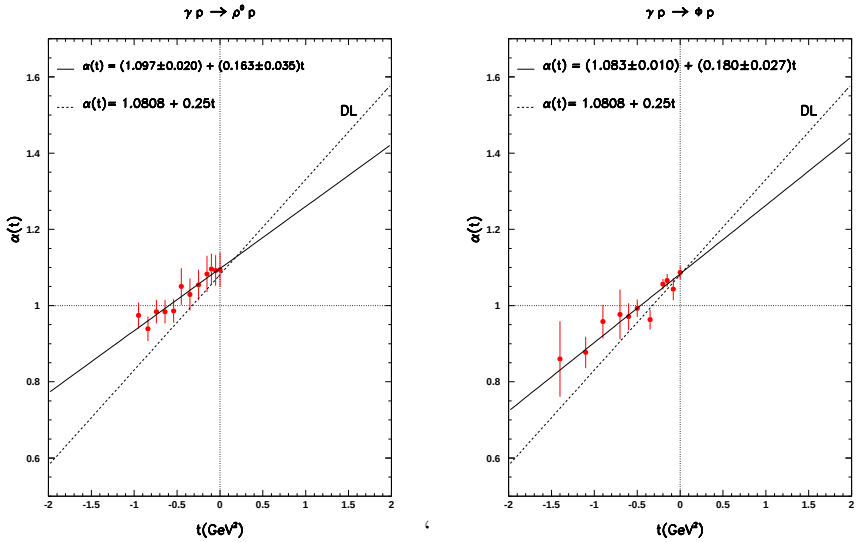

Figure 7: Preliminary results for the determination of the Pomeron trajectory in the exclusive photoproduction of ρ^0 and ϕ mesons by the ZEUS collaboration.[39] The error bars show the statistical uncertainties in the fits to the HERA data and the low-energy data as shown for the ρ^0 in Fig. 6. The result of a fit to a linear trajectory (solid line) is compared to the trajectory determined by Donnachie and Landshoff using hadronic interaction cross sections [10] (dashed line)

5.2 Exclusive electroproduction of vector mesons

Investigation of the exclusive electroproduction of ρ^0 mesons provides information on the rôle of the photon virtuality in establishing a hard scale, since we know from measurements described in the previous section that ρ^0 photoproduction at low $|t|$ can be described by a soft diffractive production mechanism. For example, the proposed perturbative description of this process implies an energy dependence which increases with photon virtuality, following the behavior of the gluon density in the proton as measured in the inclusive ep scattering process. Accurate measurements at high Q^2 have been difficult at HERA owing to statistical limitations. The H1 [48,49] and ZEUS [50] collaborations have

published measurements based on samples of a few thousand events. Figure 8 shows the energy dependence of the cross sections for exclusive ρ^0 electroproduction at various values of Q^2, comparing the fixed-target measurements at low energy [51,52] to those by the H1 [48b] and ZEUS [50] collaborations. The im-

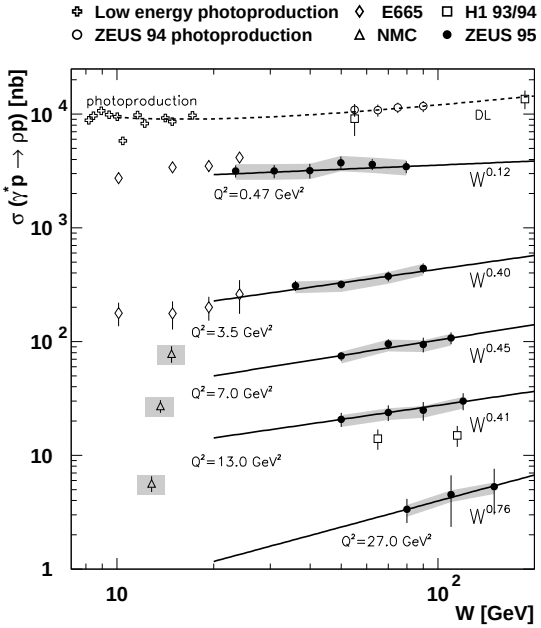

Figure 8: Comparison of cross sections for exclusive ρ^0 electroproduction as a function of W for various values of Q^2. The error bars represent statistical and systematic errors added in quadrature. The solid lines represent results of fits to the ZEUS data.[50] The dashed line is the prediction for the total photon-proton cross section by Donnachie and Landshoff.[10] The overall normalization uncertainties are shown as shaded bands for the NMC and ZEUS data points. The NMC,[51] E665 [52] and H1 [48] data points were interpolated to the indicated Q^2 values

portant question of whether the energy dependence steepens with increasing Q^2 cannot be definitively resolved at the present level of statistical accuracy. Worse yet, this QCD prediction actually holds only for the longitudinal cross section,[14,20] whereas here we consider the sum of longitudinal and transverse cross sections. Extraction of the longitudinal contribution requires the measurement of $R \equiv \sigma_{\rm L}/\sigma_{\rm T}$ (to be described in Sect. 5.3), introducing an addi-

[b]The H1 data shown here have since been superseded by their more recent measurements.[49] The new results are without consequence for our present discussion of the need for more measurements at low energy.

tional source of uncertainty.[50] The desired increase in sensitivity to the energy dependence obtained by the inclusion of the low-energy measurements suffers from an apparent discrepancy between the results at $Q^2 = 3.5\,\mathrm{GeV}^2$ from the E665 and NMC collaborations. More accurate measurements at low energy, of sufficient precision to accurately extract the longitudinal cross section, are of paramount importance for progress on this issue.

The exclusive electroproduction of J/ψ mesons has been investigated recently by both the H1 [53] and ZEUS [50] collaborations in order to shed light on the relationship between Q^2 and $M_{J/\psi}$ in determining the scale of the reaction. While experiments at the EPIC collider will not attain the high Q^2 values reached by the HERA experiments, the high luminosity at EPIC will permit accurate measurements of J/ψ electroproduction well into the perturbative regime, thus providing together with the results from HERA the long lever arm in energy which is essential for the understanding of the diffractive production process.

5.3 Helicity analyses

The simplicity of the final state in these exclusive processes permits detailed investigations of the decay-angle distributions, which have provided much information on the helicity structure of the diffractive production mechanism. The limited extent of the accessible range in y precludes the separation of longitudinal and transverse cross sections unless the proton beam energy is varied,[c] which has not yet been done at HERA. Thus the analysis of the decay-angle distributions has been employed as a means of measuring R. This type of analysis provided another early success of the perturbative QCD models of exclusive diffractive processes by verifying the prediction that the longitudinal cross section exceed the transverse cross section at high Q^2.

Three angles suffice to completely describe the exclusive electroproduction of vector mesons, as shown in Fig. 9: the azimuthal angle between the scattering plane and the production plane, Φ_h, and the two ρ^0 decay angles: ϕ_h, the azimuthal angle between the production and decay planes, defined in either the virtual-photon/proton system or in the ρ^0 rest frame, and θ_h, which is the polar angle of the positively charged decay product, defined with respect to the direction of the ρ^0 momentum vector in the virtual-photon/proton system, which is the same direction as that opposite to the momentum vector of the final-state proton in the rest frame of the ρ^0 meson. This latter choice of spin-quantization axis defines the helicity frame, in which helicity conservation was found to hold approximately in exclusive ρ^0 photoproduction experiments at

[c] This will also be the case at the EPIC collider.

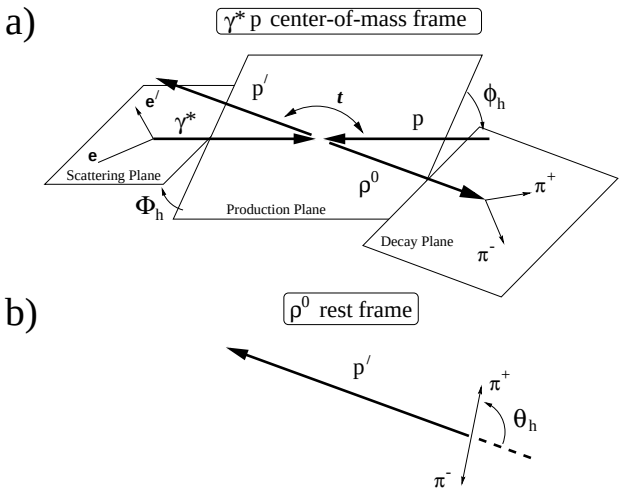

Figure 9: Schematic diagram of the process $ep \to e\rho^0 p$ (a) in the virtual-photon/proton center-of-mass system, and (b) in the rest frame of the ρ^0 meson

SLAC in the early 1970s.[54,55]

Following the work of Schilling and Wolf,[56] the three-dimensional angular distribution has been parametrized as follows:

$$
\begin{aligned}
W(\theta_h,\phi_h,\Phi_h) = \frac{3}{4\pi}\Bigg[& \frac{1}{2}(1-r^{04}_{00}) + \frac{1}{2}(3r^{04}_{00}-1)\cos^2\theta_h \\
& -\sqrt{2}\ \mathrm{Re}\{r^{04}_{10}\}\sin 2\theta_h \cos\phi_h - r^{04}_{1-1}\sin^2\theta_h\cos 2\phi_h \\
& -\epsilon\cos 2\Phi_h(r^1_{11}\sin^2\theta_h + r^1_{00}\cos^2\theta_h - \sqrt{2}\ \mathrm{Re}\{r^1_{10}\}\sin 2\theta_h\cos\phi_h \\
& \qquad -r^1_{1-1}\sin^2\theta_h\cos 2\phi_h) \\
& -\epsilon\sin 2\Phi_h(\sqrt{2}\ \mathrm{Im}\{r^2_{10}\}\sin 2\theta_h\sin\phi_h + \mathrm{Im}\{r^2_{1-1}\}\sin^2\theta_h\sin 2\phi_h) \\
& +\sqrt{2\epsilon(1+\epsilon)}\cos\Phi_h(r^5_{11}\sin^2\theta_h + r^5_{00}\cos^2\theta_h \\
& \qquad -\sqrt{2}\ \mathrm{Re}\{r^5_{10}\}\sin 2\theta_h\cos\phi_h - r^5_{1-1}\sin^2\theta_h\cos 2\phi_h) \\
& +\sqrt{2\epsilon(1+\epsilon)}\sin\Phi_h(\sqrt{2}\ \mathrm{Im}\{r^6_{10}\}\sin 2\theta_h\sin\phi_h \\
& \qquad +\mathrm{Im}\{r^6_{1-1}\}\sin^2\theta_h\sin 2\phi_h)\Bigg], \qquad (3)
\end{aligned}
$$

where the superscripts of the combinations of spin-density matrix elements correspond to the helicity degrees of freedom of the virtual photon, and the subscripts to those of the dipion state. When the dipion state is spin 1, the fifteen coefficients r^{04}_{ik}, r^{α}_{ik} are related directly to various combinations of the

helicity amplitudes, $T_{\lambda_\rho \lambda_\gamma}$, where λ_ρ and λ_γ are the helicities of the ρ^0 meson and of the photon, respectively. The assumption that helicity is conserved in the photon/vector-meson transition when the amplitudes are defined in the helicity frame ("s-channel helicity conservation" or "SCHC"), with the consequence that the degree of ρ^0 polarization is equal to the ratio of the longitudinal and transverse cross sections, allows the extraction of this ratio R from the distribution in polar angle alone. A compilation of determinations of R via this method is shown in Fig. 10. The data from the fixed-target muon experiment at FNAL, E665,[52] and the low-Q^2 data from the ZEUS collaboration identify a region of transition to increasing values of R, with the longitudinal cross section becoming dominant for $Q^2 \gtrsim 2$ GeV^2. The latest results from the H1 collaboration [49] indicate that the steep rise observed at intermediate values of Q^2 does not persist at high Q^2.

The ZEUS [57] and H1 collaborations [49] have recently completed analyses of the three-dimensional angular distribution for data samples of a few thousand events, extracting the fifteen coefficients r^{04}_{ik}, r^{α}_{ik}. Figure 11 shows the results from the ZEUS collaboration in the kinematic region $3 < Q^2 < 30$ GeV^2, $40 < W < 120$ GeV and $|t| < 0.6$ GeV^2, comparing them to the results from the H1 collaboration in a similar kinematic region, and to a calculation by Ivanov and Kirschner [18] (solid line). The inner error bars represent the statistical

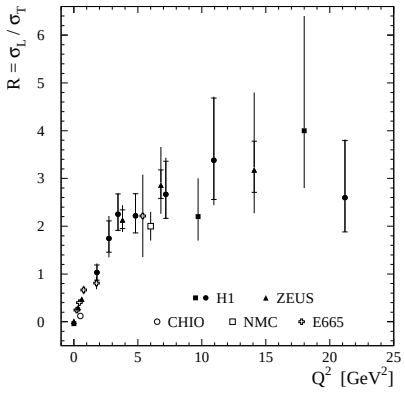

Figure 10: Measurements of the ratio of exclusive ρ^0 electroproduction cross sections for longitudinal and transverse photons, R, as a function of photon virtuality, Q^2

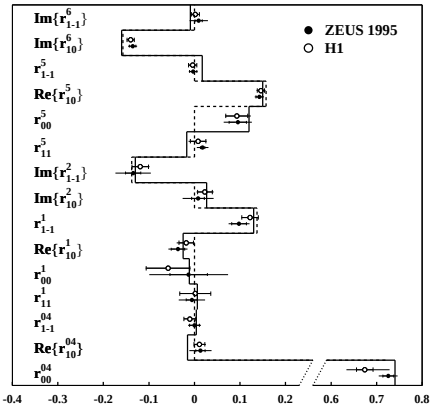

Figure 11: Combinations of spin-density matrix elements measured for ρ^0 electroproduction in the kinematic region $3 < Q^2 < 30$ GeV^2, $40 < W < 120$ GeV and $|t| < 0.6$ GeV^2 by the ZEUS collaboration.[57] See text for full description

uncertainty; the outer error bars show the quadratic sum of statistical and systematic uncertainties. Also shown are the values of the coefficients predicted according to the hypothesis of helicity conservation in the s-channel amplitudes [56] (dashed line). Of particular interest is the violation of SCHC evinced in the nonzero value for the coefficient r^5_{00}, which is manifested in the distribution in the azimuthal angle between the scattering and production planes (Φ_h). This observation implies a small nonzero single-flip amplitude for the production of ρ^0 mesons in helicity state 0 from transverse photons. Such a violation has now been reproduced in two further recent calculations based on differing assumptions.[19] These measurements show the level of violation of SCHC to be small enough that the effect of the assumption of SCHC in the earlier determinations of R is much smaller than the other sources of uncertainty in those determinations. The ZEUS collaboration also performed the analysis in the low-Q^2 region,[57] finding a value for r^5_{00} of similar magnitude, but also distinct indications for a more complex pattern of helicity violation, including double-flip contributions, as found in ρ^0 photoproduction (see Sect. 6.2).

In addition to the higher luminosity, which will allow such detailed decay-angle analyses also for J/ψ and Υ mesons, experiments at the EPIC collider will have two distinct advantages over the investigations at HERA. First, the longitudinal polarization of the electron beam will permit measurement of spin-density matrix elements currently inaccessible at HERA (namely, those of superscript 3, corresponding to circular polarization of the photon). The E665 collaboration, profiting from the longitudinal polarization of the muon beam, have published a measurement [52] of such coefficients at low Q^2. The HERA collider experiments may provide such measurements once the necessary spin rotators have been installed and the polarization program established, as is now scheduled to occur in 2001/2. The second major advantage of research at the EPIC collider is that the the polarizability of the proton beam will permit investigation of helicity flip at the nucleon vertex.[58] The H1 and ZEUS studies have no access to such information, which is essential for the complete understanding of the helicity structure of this diffractive interaction, especially for the semi-exclusive processes described below.

6 Semi-exclusive processes

The photoproduction of light vector mesons with high transverse momenta has raised interest recently [59,15,16] as a means of investigating the rôle of the momentum transfer t in establishing the scale of the interaction, since the photoproduction of ρ^0 mesons at low $|t|$ has been shown to be governed by a soft diffractive production mechanism (see Sect. 5.1). However, diffractive

photoproduction of the light vector mesons has been shown to be dominated by the proton-dissociative process for momentum transfers $|t| \gtrsim 0.5$ GeV^2 well below the perturbative regime.[39] The investigation of exclusive vector-meson production at high $|t|$ requires a trigger on the elastically scattered proton and such studies at HERA have lacked the integrated luminosity necessary to measure the small cross sections at such high values of $|t|$.[d] However, the ZEUS collaboration [60] has recently employed a photoproduction-tagging method to investigate the proton-dissociative production of ρ^0 mesons for values of $|t|$ up to 11 GeV^2. The trigger conditions required the scattered positron to be detected in a special-purpose tungsten/scintillator calorimeter located 3 cm from the positron beam axis, 44 meters distant from the nominal e^+p interaction point in the positron-beam flight direction. The position of this photoproduction tagger determines the accepted range of energy lost by the positron to the photon which interacts with the proton, thus restricting the W range to the region $80 < W < 120$ GeV. Since the transverse momentum of the final-state positron is thus required to be small ($Q^2 < 0.01$ GeV^2), the transverse momentum of the ρ^0 (p_t) detected in the central detector via its dipion decay provides an accurate approximation for the square of the momentum transferred to the proton (t): $t \simeq -p_t^2$. Offline data selection criteria include the reconstruction of exactly two tracks from the interaction vertex and reject events with calorimetric energy deposits in the rear and barrel sections of the calorimeter which are not associated with the extrapolation of either track. The selected events exhibit a semi-exclusive topology with a substantial rapidity gap between the dissociated nucleonic system and the two tracks. Even for the highest values of $|t|$, the decay pions are in the rear half of the central detector.

6.1 Differential cross sections

Differential cross sections $\frac{d\sigma}{dt}$ were obtained for ρ^0, ϕ and J/ψ mesons. Figure 12 shows the cross sections measured for ρ^0 and ϕ mesons. These exhibit an impressively hard spectrum; a fit to the form $(-t)^{-n}$ results in a value for n of approximately 3. The results are compared to a QCD calculation by Ivanov and Ginzburg [15] which estimates both perturbative and nonperturbative contributions. In this model, the nonperturbative contribution is found account for the hardness of the spectrum and to dominate in the region covered by the measurements for the ρ^0 meson. The calculation underestimates the ϕ cross section over most of the t range covered. The comparison of the data to the calculation of the perturbative contribution alone shows a good description of

[d] Clearly, a central detector together with a forward proton spectrometer at the high-luminosity EPIC collider would provide such measurements.

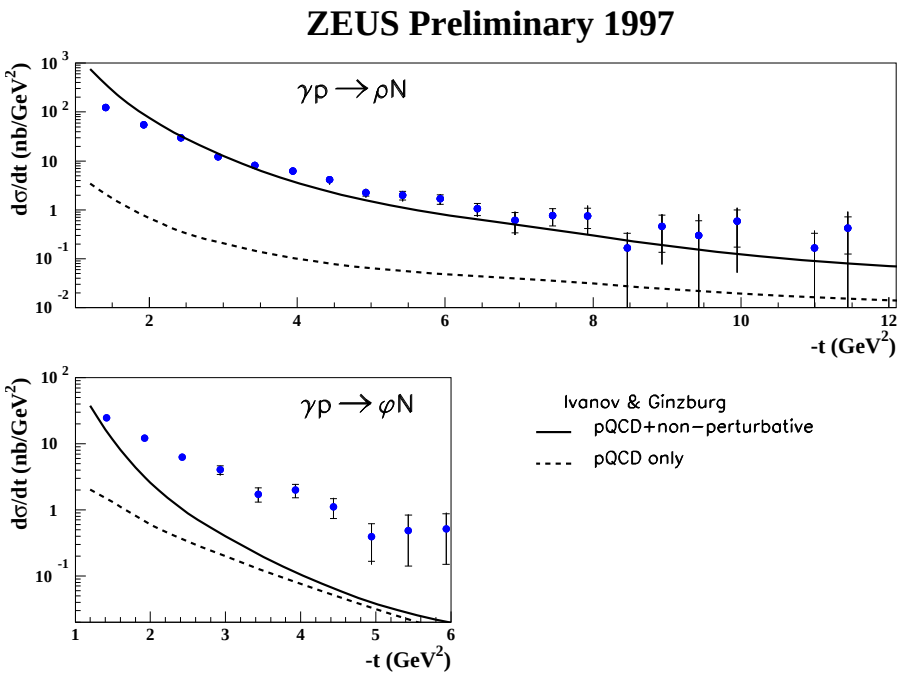

Figure 12: Preliminary measurements of the differential cross sections $\frac{d\sigma}{dt}$ for the proton-dissociative photoproduction of ρ^0 and ϕ mesons in the energy range $80 < W < 120$ GeV recently presented by the ZEUS collaboration.[60] The inner error bars represent the statistical uncertainties; the outer error bars show the quadratic sum of statistical and systematic uncertainties. The results of a QCD calculation by Ivanov and Ginzburg [15] (solid line) which distinguishes the perturbative contribution (dashed line) are shown for comparison

the shape of the t dependence, whereas the magnitude of the cross section is underestimated by more than one order of magnitude. The model thus fails to reproduce the ratio of ϕ production to that for the ρ^0 meson at high $|t|$, which is measured to be consistent with the value of 2/9 expected according to the assumption of a direct point-like coupling of the photon to the quark constituents of the vector mesons.[60] These measurements thus permit sensitive tests of perturbative models and provide information on the internal structure of the vector mesons.

6.2 Helicity analyses

The ZEUS collaboration has employed this photoproduction-tagging technique to perform decay-angle analyses of diffractive photoproduction [61,60] of pion

pairs in the ρ^0 mass region at values of $|t|$ up to 4 GeV^2. In this study, the small contribution from the elastic process was not subtracted. The decay-angle distribution was parametrized in terms of combinations of spin-density matrix elements in the Schilling-Wolf convention,[56] r^{04}_{ij}, as

$$W(\theta_h,\phi_h) = \frac{3}{4\pi}\Bigg[\frac{1}{2}\left(1-r^{04}_{00}\right)+\frac{1}{2}\left(3r^{04}_{00}-1\right)\cos^2\theta_h \\ -\sqrt{2}\mathrm{Re}(r^{04}_{10})\sin 2\theta_h\cos\phi_h - r^{04}_{1-1}\sin^2\theta_h\cos 2\phi_h\Bigg], \tag{4}$$

where the three-dimensional distribution (Eq. 3) has been averaged over the unmeasured azimuthal angle between the positron scattering plane and the ρ^0 production plane, and thus no longer distinguishes the photon helicity states ± 1.

Under the assumption that the dipion final state is produced with one unit of angular momentum, and neglecting the contribution by longitudinal photons, these combinations of matrix elements are related to the helicity amplitudes, $T_{\lambda_\rho\lambda_\gamma}$, as follows[56,57]:

$$r^{04}_{00} \simeq \frac{T^2_{01}}{T^2_{01}+T^2_{11}+T^2_{1-1}}, \qquad r^{04}_{1-1} \simeq \frac{\mathrm{Re}(T_{11}T^*_{1-1})}{T^2_{01}+T^2_{11}+T^2_{1-1}},$$

$$\mathrm{Re}(r^{04}_{10}) \simeq \frac{1}{2}\left[\frac{\mathrm{Re}(T_{11}T^*_{01})+\mathrm{Re}(T_{1-1}T^*_{0-1})}{T^2_{01}+T^2_{11}+T^2_{1-1}}\right]. \tag{5}$$

Figure 13 shows the results for the combinations of matrix elements obtained from a least-squares minimization procedure in which they served as fit parameters. The inner error bars represent the statistical uncertainty; the outer error bars show the quadratic sum of statistical and systematic uncertainties. The systematic uncertainties are dominated by the uncertainty in the acceptance corrections. The dipion mass range was restricted to the region $0.45 < M_{\pi\pi} < 1.1$ GeV. The results are compared to the results at lower $|t|$ for the exclusive reaction obtained with 9 GeV photons from a backscattered laser beam incident on a hydrogen bubble chamber at SLAC.[55] Also shown are the ZEUS 1994 results for exclusive ρ^0 photoproduction at low $|t|$.[41] The parameter r^{04}_{00} is consistent with zero over the entire range in $|t|$. The combination Re r^{04}_{10}, which is predominantly sensitive to the interference between the helicity-conserving amplitude and the single-flip amplitude, shows slight evidence for a single-flip contribution in both the SLAC data and the high-$|t|$ ZEUS results. A clear indication of a double-flip contribution is shown by the measurements of r^{04}_{1-1} at high $|t|$, as was seen in the SLAC results at lower $|t|$.

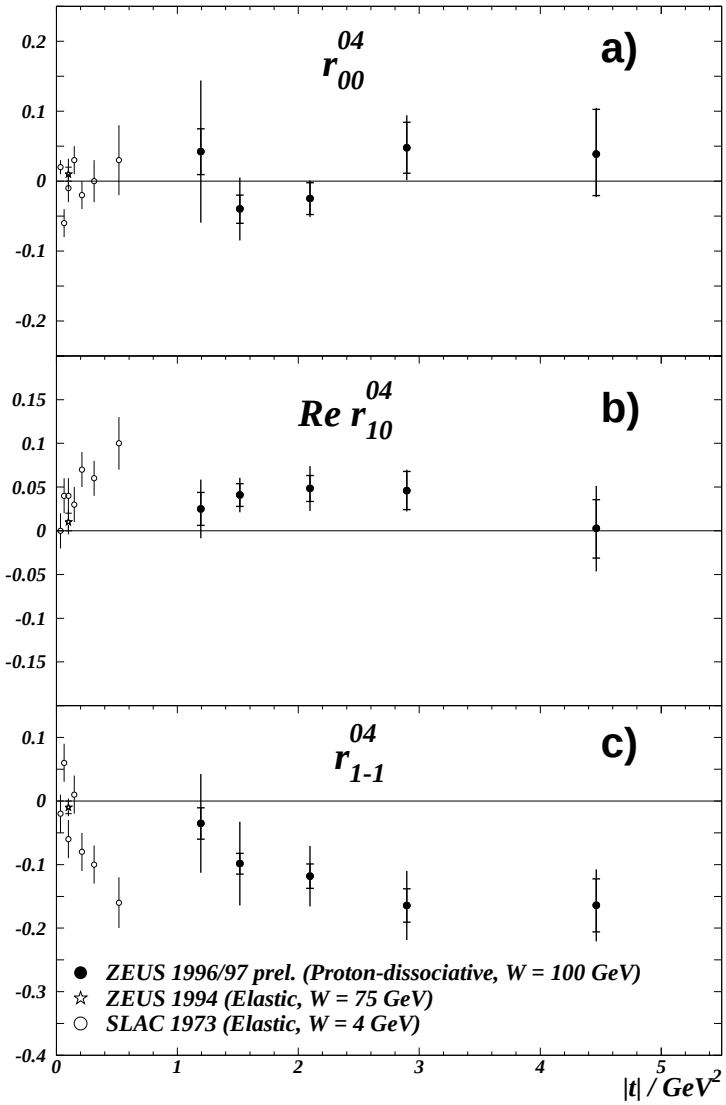

Figure 13: Recent measurements by the ZEUS collaboration [61,60] of the combinations of matrix elements (a) r_{00}^{04}, (b) Re r_{10}^{04}, (c) r_{1-1}^{04} for the diffractive photoproduction of pion pairs. The inner error bars represent the statistical uncertainties; the outer error bars show the statistical and systematic uncertainties added in quadrature. See text for full description

In order to estimate the effect on the angular distributions of a hypothesized dipion background to ρ^0 decay, the decay-angle analysis was repeated for restricted dipion mass ranges above ($0.77 < M_{\pi\pi} < 1.0$ GeV) and below ($0.6 < M_{\pi\pi} < 0.77$ GeV) the nominal value for the ρ^0 mass. The observed value for each of the combinations of matrix elements was found to depend significantly on the mass range chosen, though the above conclusions concerning the lack of longitudinal polarization and the evidence for a double-flip contribution remain unchanged. This dependence on dipion invariant mass may suggest the presence of a nonresonant background. The extraction of the spin-density matrix elements for the ρ^0 meson alone from these dipion angular distributions thus awaits the understanding of this dependence.

The complexity of this helicity structure, which the SLAC results showed to hold also at an energy lower than that of EPIC, is thus shown to persist at high values of $|t|$ where the hardness of the $|t|$ spectrum and the ϕ/ρ^0 ratio encourage attempts to describe this semi-exclusive process in the framework of perturbative QCD. The physics program at the EPIC collider, which emphasizes high luminosity and polarizability over high energy, will permit the conclusive resolution of these fundamental quandaries in the understanding of the strong interaction.

7 Concluding remarks

This report has presented a selection of investigations by the H1 and ZEUS collaborations into diffractive processes in electron-proton interactions, using results obtained during the first six years of operation of the HERA collider. These studies have provided a great deal of information pertaining to the applicability of quantum chromodynamical descriptions of diffraction. Particular emphasis has been placed on relevance to the physics program at the proposed EPIC electron/polarized-ion collider, bringing investigations which require a wide energy range within the asymptotic region at high energy, and those of the helicity structure of diffraction to the fore. The rich phenomenology of examples of inclusive, exclusive and semi-exclusive processes in electron-proton interactions has been discussed. However, this synopsis cannot pretend to have been an exhaustive list of the open questions which are to be addressed by experiments at the EPIC collider, not even of those which have already begun to be investigated at HERA. One need merely consider the issues of the dependence of the exponential slopes in t at low $|t|$ on energy and photon virtuality in both exclusive and semi-exclusive processes, of vector-meson production ratios, of photo- and electroproduction of radially excited quarkonia and of production processes involving the exchange of quantum numbers

other than those of the vacuum to recognize the incompleteness of the present summary. The experimental program of the collider experiments at HERA has made obvious the power of such investigations to elucidate the properties of the strong interaction. Experimental investigations at the EPIC collider are certain to provide high statistical accuracy in the kinematic region which must be further investigated in order to make progress in our understanding of strong-interaction dynamics.

Acknowledgments

The author gratefully acknowledges support from the workshop organizers. This work is also supported by the Federal Ministry of Education and Research of Germany.

1. A. Schäfer and D. von Harrach, GSI-Report 98-04, Report of the Joint DESY/GSI/NuPECC Workshop *Electron-Nucleon/Nucleus Collisions*, March 1997, Seeheim, Germany.
2. M. Diehl, LANL Preprint hep–ph/9906518 (1999), review talk held at the 7th International Workshop on Deep Inelastic Scattering and QCD (DIS99), Zeuthen, Germany, 19-23 April 1999.
3. *Proceedings of the Workshop on Physics at HERA*, edited by W. Buchmüller and G. Ingelman (DESY, Hamburg, Germany, 1992).
4. J. A. Crittenden, *Exclusive Production of Neutral Vector Mesons at the Electron-Proton Collider HERA,* Springer Tracts in Modern Physics, Volume 140 (Springer, Berlin Heidelberg, 1997).
5. M. Strikman, these proceedings.
6. L. Frankfurt and M. Strikman, LANL Preprint hep–ph/9907221 (1999).
7. G. Piller and W. Weise, LANL Preprint hep–ph/9908230 (1999).
8. P.D.B. Collins, *An Introduction to Regge Theory and High-Energy Physics* (Cambridge University Press, 1977).
9. H. Abramowicz and A. Caldwell, DESY Report 98–192 (1998), LANL preprint hep-ex/9903037, to be published in *Reviews of Modern Physics*.
10. A. Donnachie and P.V. Landshoff, Phys. Lett. **B296** (1992) 227.
11. V. N. Gribov, Sov. Phys. JETP **14** (1962) 478, Original: JETP **41** (1961) 667.
12. F.E. Low, Phys. Rev. **D12** (1975) 163; S. Nussinov, Phys. Rev. Lett. **34** (1975) 1286; S. Nussinov, Phys. Rev. **D14** (1976) 246.
13. H. Abramowicz, L. Frankfurt and M. Strikman, Surveys in High-Energy Physics **11** (1997) 51, DESY Report 95–047, LANL preprint hep–ph/9503437.
14. S. J. Brodsky *et al.*, Phys. Rev. **D50** (1994) 3134.

15. D. Yu. Ivanov, Phys. Rev. **D53** (1996) 3564; I. F. Ginzburg and D. Yu. Ivanov, Phys. Rev. **D54** (1996) 5523.
16. S. J. Brodsky, M. Diehl, P. Hoyer and S. Peigné, Phys. Lett. **B449** (1999) 306.
17. S. J. Brodsky, these proceedings.
18. D. Yu. Ivanov and R. Kirschner, Phys. Rev. **D58** (1998) 114026.
19. Talks by I. Royen and N. Nikolaev, 7th International Conference on Deep Inelastic Scattering and QCD, 19-23 April, 1999, Zeuthen, Germany.
20. J. C. Collins, L. Frankfurt and M. Strikman, Phys. Rev. **D56** (1997) 2982.
21. A. Hebecker, LANL Preprint hep–ph/9905226 (1999).
22. M. G. Ryskin, Z. Phys. **C57** (1993) 89.
23. L. Frankfurt, W. Koepf and M. Strikman, Phys. Rev. **D54** (1996) 3194.
24. B. Humpert and A.C.D. Wright, Phys. Lett. **B65** (1976) 463; B. Humpert and A.C.D. Wright, Phys. Rev. **D15** (1977) 2503.
25. F. Gilman, Phys. Rev. **167** (1968) 1365; L. Hand, Phys. Rev. **129** (1963) 1834.
26. B.L. Ioffe, V.A. Khoze, and L.N. Lipatov, *Hard Processes* (North Holland, Amsterdam, 1984).
27. ZEUS Collaboration, M. Derrick *et al.*, Z. Phys. **C72** (1996) 399.
28. H1 Collaboration, Nucl. Phys. **B470** (1996) 3.
29. NMC Collaboration, M. Arneodo *et al.*, Phys. Lett. **B364** (1995) 107.
30. H. Abramowicz *et al.*, Phys. Lett. **B269** (1991) 465; A. Marcus, *Energy Dependence of the* γ^*p *Cross Section*, Master's thesis, Tel-Aviv University, 1996.
31. ZEUS Collaboration, J. Breitweg *et al.*, Paper submitted to the XXIX International Conference on High-Energy Physics, 23-29 July 1998, Vancouver, Canada (Abstract 789).
32. H1 Collaboration, C. Adloff *et al.*, Eur. Phys. J. **C6** (1999) 587.
33. A. D. Martin, M. G. Ryskin, T. Teubner, Phys. Lett. **B454** (1999) 339.
34. L. L. Frankfurt, M. F. McDermott and M. Strikman, LANL preprint hep–ph/9812316 (1998).
35. ZEUS Collaboration, M. Derrick *et al.*, Z. Phys. **C69** (1995) 39.
36. H1 Collaboration, C. Adloff *et al.*, Paper submitted to the International Europhysics Conference on High-Energy Physics, 15–21 July, 1999, Tampere, Finland (Paper 157aj).
37. M. G. Ryskin, R. G. Roberts, A. D. Martin and E. M. Levin, Z. Phys. **C76** (1997) 231; L. Frankfurt, W. Koepf and M. Strikman, Phys. Rev. **D57** (1998) 512.
38. A. Levy, Phys. Lett. **B424** (1998) 191.

39. ZEUS Collaboration, J. Breitweg *et al.*, Paper submitted to the XXIX International Conference on High-Energy Physics, 23-29 July 1998, Vancouver, Canada (Abstract 788).
40. H1 Collaboration, S. Aid *et al.*, Nucl. Phys. **B463** (1996) 3.
41. ZEUS Collaboration, J. Breitweg *et al.*, Eur. Phys. J. **C2** (1998) 247.
42. ZEUS Collaboration, M. Derrick *et al.*, Z. Phys. **C73** (1997) 253.
43. D. Aston *et al.*, Nucl. Phys. **B 209** (1982) 56.
44. J. R. Cudell *et al.*, LANL Preprint hep–ph/9908218 (1999).
45. A. Donnachie and P. V. Landshoff, Phys. Lett. **B231** (1984) 189.
46. EMC Collaboration, J. J. Aubert *et al.*, Nucl. Phys. **B213** (1983) 1.
47. H1 Collaboration, C. Adloff *et al.*, Paper submitted to the XXIX International Conference on High-Energy Physics, 23-29 July 1998, Vancouver, Canada (Abstract 572).
48. H1 Collaboration, S. Aid *et al.*, Nucl. Phys. **B468** (1996) 3.
49. H1 Collaboration, C. Adloff *et al.*, DESY Report 99-010 (1999), LANL Preprint hep-ex/9902019, to appear in Eur. Phys. J.
50. ZEUS Collaboration, J. Breitweg *et al.*, Eur. Phys. J. **C6** (1999) 603.
51. NMC Collaboration, M. Arneodo *et al.*, Nucl. Phys. **B429** (1994) 503.
52. E665 Collaboration, M. R. Adams *et al.*, Z. Phys. **C74** (1997) 237.
53. H1 Collaboration, C. Adloff *et al.*, DESY Report 99-026 (1999), LANL Preprint hep-ex/9903008, to appear in Eur. Phys. J.
54. J. Ballam *et al.*, Phys. Rev. **D5** (1972) 545.
55. J. Ballam *et al.*, Phys. Rev. **D7** (1973) 3150.
56. K. Schilling and G. Wolf, Nucl. Phys. **B61** (1973) 381.
57. ZEUS Collaboration, J. Breitweg *et al.*, DESY Report 99-102 (1999), LANL Preprint hep-ex/9908026, submitted to Eur. Phys. J.
58. M. Diehl, LANL Preprint hep–ph/9907568 (1999), review talk held at Nucleon'99, Frascati, Italy, 7-9 June 1999.
59. J. Bartels, J. R. Forshaw, H. Lotter and M. Wüsthoff, Phys. Lett. **B375** (1996) 301.
60. ZEUS Collaboration, J. Breitweg *et al.*, Paper submitted to the International Europhysics Conference on High-Energy Physics, 15–21 July, 1999, Tampere, Finland (Abstract 499).
61. J. A. Crittenden for the ZEUS Collaboration, contributed to the proceedings of the 7th International Conference on Deep Inelastic Scattering and QCD, 19-23 April, 1999, Zeuthen, Germany, LANL preprint hep-ex/9906005.